Altered expression of expansin modulates leaf growth and pedicel abscission in *Arabidopsis thaliana*

Hyung-Taeg Cho* and Daniel J. Cosgrove

Department of Biology, 208 Mueller Laboratory, Pennsylvania State University, University Park, PA 16802

Expansins are cell-wall-loosening proteins that induce stress relaxation and extension of plant cell walls. To evaluate their hypothesized role in cell growth, we genetically manipulated expansin gene expression in *Arabidopsis thaliana* and assessed the consequent changes in growth and cell-wall properties. Various combinations of promoters were used to drive antisense and sense sequences of *AtEXP10*, which is maximally expressed in the growing leaf and at the base of the pedicel. Compared with controls, antisense lines had smaller rosettes because of shorter petioles and leaf blades and often acquired a twisted leaf morphology. Petiole cells from antisense plants were smaller than controls and their cell walls were significantly less extensible *in vitro*. Sense plants had slightly longer petioles, larger leaf blades, and larger cells than controls. Abscission at the base of the pedicel, where *AtEXP10* is endogenously expressed, was enhanced in sense plants but reduced in antisense lines. These results support the concept that expansins function endogenously as cell-wall-loosening agents and indicate that expansins have versatile developmental roles that include control of organ size, morphology, and abscission.

antisense | AtEXP10 | cell growth | cell wall | extracellular matrix

The plant extracellular matrix is dominated by the cell wall, which in growing cells consists of a pliant network of cellulose microfibrils embedded in a matrix of neutral and acid polysaccharides and minor structural proteins (1, 2). The enlargement of plant cells requires shear (slippage) of the structural polymers within the cell wall, which must simultaneously maintain sufficient strength to withstand high turgor forces. Although cell wall hydrolases and transglycosylases are notably involved in disassembly of the cell wall during fruit ripening and organ abscission (3–5), their importance for cell-wall enlargement is less clear. Another class of wall protein, named expansin, has the unique ability of inducing cell-wall extension without hydrolytic breakdown of the major structural components of the cell wall (1, 6). Previous work has implicated expansin as a control factor for cell growth, based on experiments in which exogenous protein was applied to isolated cell walls and to living cells (7–10). These studies support the concept that expansin protein serves as a wall-loosening agent to promote cell enlargement. Additionally, gene expression studies indicate that expansin transcript abundance is greatest during cell growth and during fruit softening and moreover is modulated by hormones and environmental stimuli in a manner consistent with its putative role in cell growth (11–15).

Expansin genes have been identified in a range of land plants including bryophytes (R. Carey and D.J.C., unpublished data), ferns (J.-H. Kim, H.-T.C., and H. Kende, unpublished data), gymnosperms (16), and diverse angiosperms (17). Expansins make up a large superfamily that is divided into two major families, α- and β-expansins, on the basis of sequence divergence and biochemical activity (1). With nearly 30 expansin genes in *Arabidopsis* (http://www.bio.psu.edu/expansins/), the possibility for redundancy and overlapping expression presents serious limitations to functional analysis by reverse genetics (18). In a first attempt to modify expansin expression by use of the 35S cauliflower mosaic virus (CaMV) promoter to drive expression of full-length expansin genes, *Arabidopsis* transformants showed complicated and unstable phenotypes, apparently caused by gene silencing (T. Y. Shcherban and D.J.C., unpublished results). To circumvent this problem, we have examined the specific role of *Arabidopsis* expansin-10 (AtEXP10) by manipulating gene expression in a tissue-specific way. Our results support the hypothesis that endogenous expansin plays a role in cell enlargement, organ morphogenesis, and abscission, roles that are consistent with the biophysical and growth effects observed when expansin protein is applied to isolated cell walls and living plant cells.

Materials and Methods

Plant Material. *Arabidopsis thaliana* (L.) Heynh (ecotype Columbia) plants were grown on soil medium at 23°C under 12 h light/12 h dark. For selection of transgenic plants, seeds were sterilized in ethanol and bleach, rinsed with water, and germinated on agar medium containing 10 μg/ml hygromycin. Hygromycin-resistant seedlings were transferred to soil medium.

Transgene Constructs. The *AtEXP10* gene (GenBank accession no. AF229431) was isolated from a lambda phage genomic library (T. Y. Shcherban, D. M. Durachko, and D.J.C., unpublished data). Its structure is shown in Fig. 1*A*. The corresponding cDNA (GenBank accession no. AF229437) was cloned by reverse transcription (RT)-PCR with primers 5′-ACGAAGAGCTC-CAAGTCCCAAG-3′ and 5′-ATTGAGCTCCCGGG(T)$_{17}$-3′ and total RNA from young leaves. The TATA box and transcription initiation site were predicted with the WEBGENE program (http://www.itba.mi.cnr.it/webgene).

For the transformation experiments, one control construct, one *AtEXP10* sense construct, and three *AtEXP10* antisense constructs were engineered. The sense sequence was prepared by PCR using primers 5′-TTTCCCGGGTACATATTTACTT-GTG-3′ and 5′-TTAGAGCTCTTAAAGATCCTCCTCA-GAAATAAGCTTCTGCTCACGGAACTG TCCACC-3′; these primers direct amplification of the whole coding region between bases 120 and 1,078 of the genomic *AtEXP10*. The PCR fragment was digested with *Xma*I and *Sac*I and inserted into the binary vector pGPTV-HPT (19) by replacing *uid-A* between the *Xma*I/*Sma*I and *Sac*I/*Sst*I sites. The *AtEXP10* promoter region (1,525 bp) between bases −1,470 and 55 then was inserted into
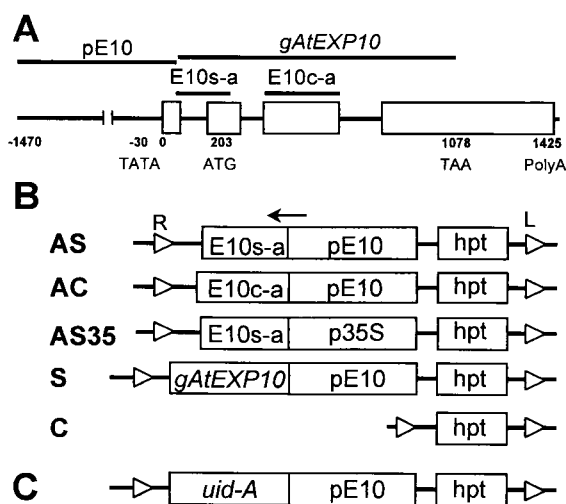
Fig. 1. Structure of *AtEXP10* and antisense, sense, and control constructs for *Arabidopsis* transformation. (*A*) Gene structure of *AtEXP10*. Open boxes represent exons. E10s-a and E10c-a indicate the regions from which antisense sequences were prepared for AS (or AS35) and AC, respectively. A sense sequence was prepared from *gAtEXP10*. pE10 represents the promoter region of *AtEXP10*. (*B*) Transgene constructs. AS, antisense construct specific to *AtEXP10* (E10s-a) driven by pE10; AC, antisense construct containing *AtEXP10* coding region (E10c-a) and driven by pE10; AS35, antisense construct specific to *AtEXP10* (E10s-a) driven by 35S CaMV promoter (p35S); S, sense construct containing genomic *AtEXP10* (*gAtEXP10*) and driven by pE10; C, control construct containing only hygromycin phosphotransferase gene cassette (hpt) as a selectable marker. Small open triangles at the end of the each line represent right border (R) and left border (L) of the T-DNA in *Agrobacterium* Ti (tumor-inducing) plasmid. The arrow indicates the direction of transcription. (*C*) The construct for expression of GUS driven by pE10 (*AtEXP10*::GUS).

the *Sma*I site of this vector (the final sense construct, S, in Fig. 1*B*). For the *AtEXP10*-specific antisense constructs AS and AS35, the gene-specific region containing the 5′ untranslated region and the signal peptide sequence from the genomic *AtEXP10* was amplified with primers 5′-ACGAAGAGCTC-CAAGTCCCAAG-3′ and 5′-GTACCCGGGCACAGAA-GAAGC-3′. The 200-bp fragment was inserted between the *Xma*I and *Sac*I sites of pGPTV-HPT in antisense orientation. For the AS construct, the *AtEXP10* promoter was inserted before the antisense sequence as described for the S construct. For the AS35 construct, the 35S CaMV promoter, excised by *Hin*dIII and *Xba*I from pBI121 (Clontech), was used to drive the *AtEXP10*-specific antisense expression. A gene fragment for another antisense construct, AC, containing the conserved coding region was produced from the third exon of genomic *AtEXP10* by PCR using primers 5′-AGGTGGAGCTCGTGGATATGG-3′ and 5′-GAACCCGGGACGATTCCAGCTC-3′. This 310-bp product was inserted between *Xma*I and *Sac*I sites of pGPTV-HPT, and the *AtEXP10* promoter was inserted ahead of this antisense sequence as described for the S construct. The control construct was engineered so as to have only the *hpt* gene cassette between two borders in the binary vector. In the *AtEXP10*::GUS construct, the *AtEXP10* promoter (1,525 bp) was inserted into the *Xba*I site of pGPTV-HPT so that the promoter directs the expression of the *uid* A gene (Fig. 1*C*). All of the constructs were confirmed by DNA sequencing. The constructs were introduced into *Agrobacterium tumefaciens* strain C58C1 (pMP90), which was used to transform *Arabidopsis* by vacuum infiltration (20).

PCR. For RT-PCR, total RNA from *Arabidopsis* tissues was isolated with the RNeasy Plant Mini Kit (Qiagen). RT-PCR was performed by using the One Step RT-PCR System (Roche,

Indianapolis). The 10-μl reaction mixture was composed of 0.4 mM of each deoxynucleotide phosphate, 7% dimethyl sulfoxide, 5 mM DTT, 0.3 μM of each primer, 0.2 μl *Carboxydothermus hydrogenoformans* polymerase, and nominally 10 ng of RNA template. The amount of RNA in each sample was carefully normalized so that RT-PCR amplification of 18S rRNA resulted in a band of similar intensity on an agarose gel. For rRNA amplification, the primers were 5′-TTGTGTTGGCTTCGG-GATCGGAGTAAT-3′ and 5′-TGCACCACCACCCATA-GAATCAAGAA-3′, giving a product of ≈400 bp. The amount of *AtEXP10* mRNA was assessed by RT-PCR using gene-specific primers 5′-GAGAGATTAACCAACTTGCC-3′ and 5′-AGTACAGAGCTGGAATCGTC-3′. To detect *AtEXP10* mRNA from the S construct, an S-specific primer set was used (5′-AGTACAGAGCTGGAATCGTC-3′ and 5′-CCAAAT-GTTTGAACGATCGGGG-3′). For quantitative RT-PCR, we set up five reactions for each RNA sample and removed them from the thermocycler at consecutive cycles. Product amounts were assessed by electrophoresis in ethidium bromide-containing agarose gels, followed by photography and quantification with the histogram function in Adobe Systems (Mountain View, CA) PHOTOSHOP Version 5.0.

Detection of β-Glucuronidase (GUS) Activity. *Arabidopsis* plants containing the *AtEXP10*::GUS construct were stained with 5-bromo-4-chloro-3-indolyl-β-D-glucuronide cyclohexylammo-nium salt (0.5 mg/ml) in staining buffer (100 mM NaH$_2$PO$_4$/10 mM Na$_2$EDTA/0.5 mM potassium ferrocyanide/0.5 mM potassium ferricyanide/0.1% Triton X-100, pH 7, with NaOH) for 48 h at 37°C and were cleared in 70% ethanol for 48 h at 37°C.

Extensometer Assays. Petiole cell walls (1 cm) from the seventh leaf of 29-day-old plants were assayed with a custom-made extensometer (21). Because petiole diameters differed in the sense and antisense lines, the extensometer load was adjusted to give equal stress (force per unit area) by normalizing to wall cross-sectional area (22). Petiole cell-wall cross-sectional area was estimated as dry weight per unit length, giving values of 0.134, 0.147, and 0.101 mg/cm for the control, sense, and antisense lines, respectively. Extensometer loads were accordingly adjusted to 10, 11.1, and 7.5 g, respectively, for control, sense, and antisense lines.

Abscission Test of Pedicels. Physical abscission was conducted either by manual pulling on the pedicel or by using a force transducer with a constant strain rate of 3.7 mm/min. Both methods gave similar results. The assay was performed when the primary inflorescence stem held more than 20 siliques and the first to sixth siliques from the bottom had begun to turn yellow.

Results

Endogenous Expression of *AtEXP10*. Because preliminary trials showed that expression of expansins, including *AtEXP10*, was too low in *Arabidopsis* to be detected by RNA gel blotting with total RNA or by immunoblot analysis (data not shown), we identified the spatial and temporal expression pattern of *AtEXP10* by using *AtEXP10*::GUS and RT-PCR. The first expression detectable by *AtEXP10*::GUS occurred at the base of the emerging first two true leaves but not of the cotyledons (Fig. 2*B*). At this and later stages, a low level of staining in the shoot meristem was observed (data not shown). Diffuse staining also appeared transiently in the emerging petioles of the first leaves, but became more obvious and extended into the leaf midrib from the third leaf onward (Fig. 2*A*). As leaf development progressed, *AtEXP10*::GUS expression began in the base of the petiole and gradually extended toward the whole midrib; later, it was restricted to the vasculature of the petiole and leaf blade before it disappeared altogether as the leaf matured. *AtEXP10*::GUS also
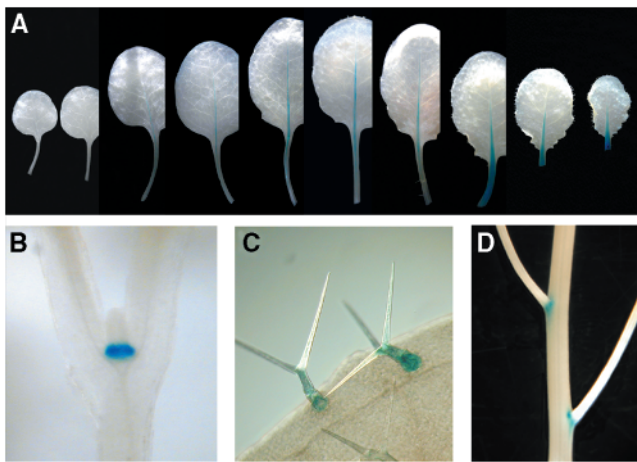
Fig. 2. Expression of *AtEXP10*::GUS in *Arabidopsis*. *AtEXP10* is expressed in the petiole and midrib [in leaves from a 29-day-old-plant (*A*)], the base of the emerging first leaves [in a 5-day-old plant (*B*)], the trichomes (*C*), and the pedicel abscission region (*D*). In *A*, leaves are arranged from the first leaf at the left.

was notably expressed in growing trichomes (epidermal hairs; Fig. 2*C*) and at the base of pedicels (Fig. 2*D*), which are the stalks connecting the flower to the inflorescence stem.

Consistent with this staining pattern, RT-PCR analysis showed much greater *AtEXP10* expression in young growing petioles and leaf blades than in older nongrowing leaves (Fig. 3*A*). We estimate ≈200-fold more *AtEXP10* mRNA in young leaf blades and ≈35-fold more *AtEXP10* mRNA in young petioles as compared with corresponding mature tissues. These estimates assume a 1.8-fold amplification per cycle (23). Similarly, the expression level was much higher (≈35-fold) in the pedicel bases when the silique was still young (green) than when it was maturing (yellow).

Although the RT-PCR results generally agreed with the *AtEXP10*::GUS staining patterns, there were two regions where RT-PCR indicated higher expression than expected based on staining by *AtEXP10*::GUS. These regions were in the leaf blade and in the inflorescence stem between the pedicel nodes (Fig. 3). RT-PCR analysis indicated the message level for *AtEXP10* in the midrib was ≈2-fold higher than in the blade tissue (Fig. 3*B*), whereas the GUS staining suggested that expression in the blade was restricted to the trichomes, which make up a small fraction of the blade. Specific *AtEXP10* expression in trichomes was confirmed by *in situ* hybridization (data not shown). It is possible that the expression in the blade detected by RT-PCR is entirely attributable to high mRNA levels in the trichomes, but we cannot exclude low-level, diffuse expression in other blade tissues as well. Likewise in the inflorescence, RT-PCR analysis indicated the message level was 2.4- to 4.3-fold higher in the pedicel bases as compared with the neighboring stem region, whereas the GUS staining suggested a greater contrast. These differences might be attributable to longevity of GUS enzyme or to additional gene-expression control elements outside the *AtEXP10* promoter. Additionally, GUS staining is not quantitative, but rather tends to emphasize the regions with highest expression.

From these results, we conclude that *AtEXP10* is most highly expressed in the young leaf petiole and midrib, in trichomes, and at the base of the pedicel.

Construction of *AtEXP10* Transformants. To examine the tissue-specific effect of expansin overexpression and suppression, we chose to drive expression with the *AtEXP10* promoter or to express an antisense sequence that is specific to *AtEXP10* and not
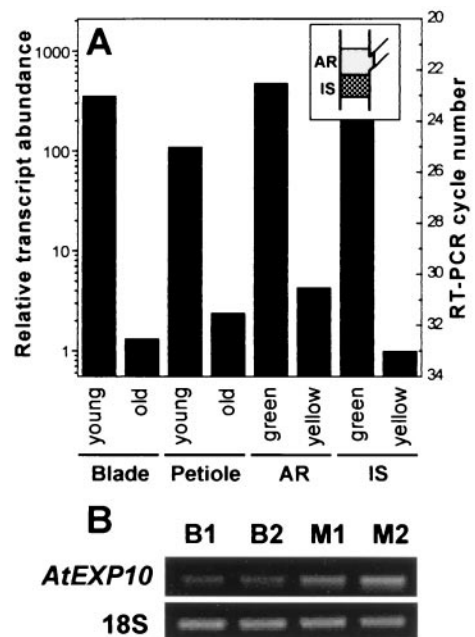

Fig. 3. RT-PCR analysis of *AtEXP10* expression in selected *Arabidopsis* tissues. (*A*) Quantitative RT-PCR analysis of the RNA from young and old leaf blades and petioles, from pedicel abscission regions (AR, see *Inset*), and from the inflorescence stems (IS) subtending AR. The young blade and petiole are from the fifth leaf of 21-day-old plants and the old ones are from the fifth leaf of 35-day-old plants. AR and IS tissues were taken when the siliques were green (young) or yellow (old). Relative transcript abundance was calculated from the minimum number of cycles needed for detection of the amplified product on an ethidium bromide-stained gel. Amplification by 1.8-fold per cycle was assumed. The minimum number of cycles is shown on the right axis and is an average of two to four repeats. (*B*) RT-PCR results of RNA from the midrib (M) and the blade (B) tissues. Total RNA of each tissue was prepared from the eighth leaf of 27-day-old plants. The numbers indicate different RNA preparations. Primers for 18S rRNA (18S) were used for an internal loading standard in *A* and *B*. In *B*, the RT-PCR cycle numbers were 29 for *AtEXP10* and 16 for 18S.

to other expansins. For this purpose, three antisense and one sense constructs were made: AS uses the *AtEXP10* promoter to control the *AtEXP10*-specific antisense sequence to suppress only *AtEXP10* expression; AC contains the antisense for the conserved coding region of the *AtEXP10* gene and is driven by the *AtEXP10* promoter to suppress *AtEXP10* plus any closely related expansins; AS35 contains the *AtEXP10*-specific antisense sequence driven by the 35S CaMV promoter, expected to have a stronger promoter activity throughout most tissues; and S contains the *AtEXP10* promoter followed by the *AtEXP10* genomic sense sequence for tissue-specific overexpression of *AtEXP10* (Fig. 1*B*). For each construct, 35 to 71 independent hygromycin-resistant primary transformants (T1) were selected for T1 analysis, and 3 to 6 T1 lines per construct were further analyzed in the T2 generation.

Integration of the transgenes into the genome was confirmed by PCR analysis of the plant DNA by using transgene-specific primers (data not shown). Antisense transcripts of AS and AC transgenes could not be detected in leaf tissue by RT-PCR, most likely because of antisense mRNA instability (24). AS35 antisense message was detectable at low level, probably because of the strong activity of the 35S CaMV promoter, and the sense (S) transcript was likewise detected by RT-PCR (data not shown).

Transgenic plants had significant changes in steady-state *AtEXP10* message levels (Fig. 4), with reductions of 50% to 96% in antisense lines and increases of 57% to 277% in sense lines, as compared with control transgenic lines.
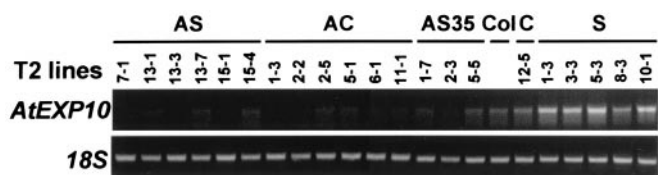
Fig. 4. RT-PCR analysis of *AtEXP10* expression in selected transgenic lines. RNA from the fifth leaf of 21-day-old T2 plants was analyzed. The RT-PCR cycle numbers were 28 for *AtEXP10* and 16 for 18S. Col, Columbia wild type.

As described below for the independent T1 lines and their progeny, antisense plants had smaller rosettes and aberrant leaves as compared with controls, whereas sense plants were slightly larger and matured earlier than did control plants. The inflorescence stems of some antisense lines tended to recline. Trichomes were not visibly altered, perhaps because of the redundant expression of other expansin genes in the trichome (D.J.C., unpublished results). Below, we characterize the most obvious phenotypic characters of the transformants, namely, altered rosette size, leaf shape, and abscission of the pedicel.

Altered Leaf Growth and Wall Properties in *AtEXP10* Transgenic Plants. T2 plants, from T1 lines with the more extreme yet still characteristic phenotype, are presented in Fig. 5 *A* and *B*, whereas the

size distributions for the full T1 populations are shown in Fig. 5*C*. The morphology of AS35 plants was similar to that of AS and AC plants (data not shown). Antisense lines were significantly smaller than controls, averaging 71% (AS), 59% (AC), and 58% (AS35) in rosette diameter as compared with the control transgenic plants. AS35 lines showed a bimodal distribution with an extremely small-sized group (1–4 cm) and a moderately small-sized group (5–7 cm). The average rosette diameter of S lines was 18% larger than that of control lines.

T1 lines with rosette size typical of the population were selfed, and hygromycin-resistant T2 plants were further analyzed (Fig. 5*D*; Table 1). Both petiole and blade lengths were modified in the T2 plants, with somewhat larger effects for the petiole, which is consistent with the expression pattern for *AtEXP10*::GUS. Growth of antisense plants diverged from that of controls early on, depending on the severity of phenotype in different lines (Fig. 5*D*). The selected AS35 lines showed much slower growth than did the other antisense lines. In the sense lines, rosette size became greater than that in controls after day 30, which is when the largest rosette leaves started to reach full size.

The cellular basis for these growth alterations was examined by measurements of cell number and cell size in petioles of T3 plants (Table 2). Cell number per file did not differ significantly. In contrast, cell length was significantly increased in the sense line and decreased in the antisense line; these changes accounted
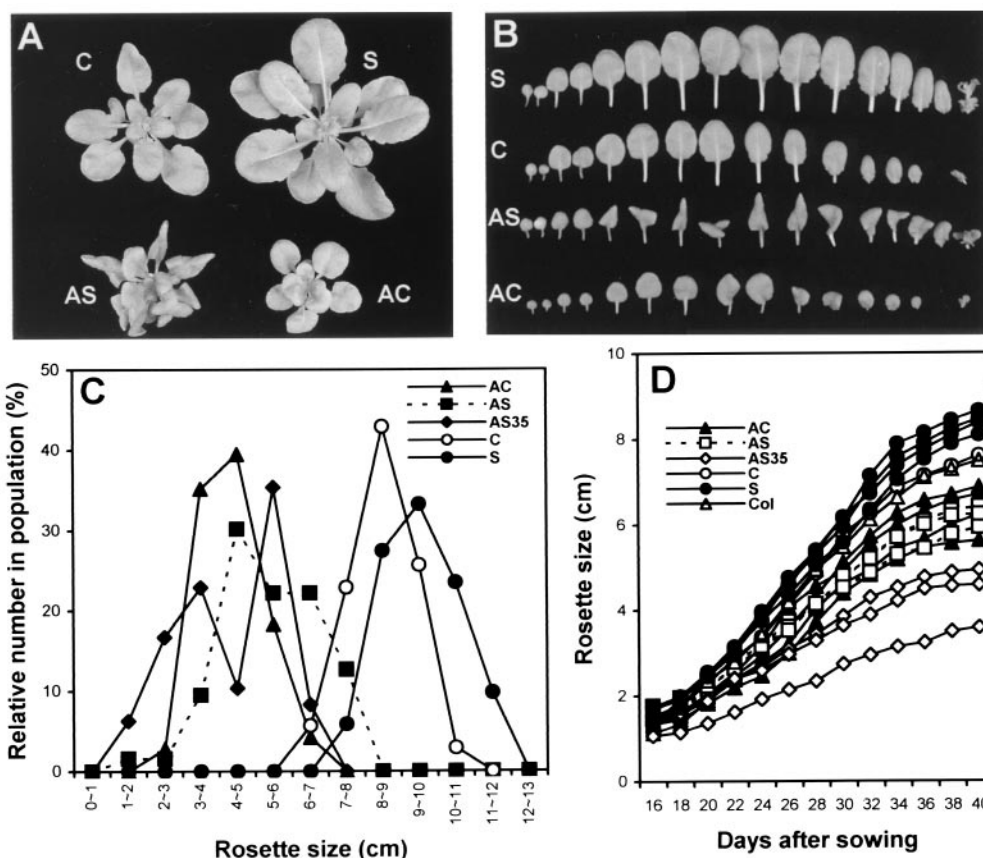

Fig. 5. Effect of *AtEXP10* transgenes on rosette and leaf growth. (*A*) Rosettes from 35-day-old T2 plants. The sense plant (S) shown here is the progeny of the T1 line with the largest rosette size (11–12 cm), as shown in Fig. 5*C*; the AS plant is from the T1 line with most severely malformed leaves; and the AC plant is from the T1 line with smallest rosette size (2–3 cm) but with mildly deformed leaves. (*B*) Alignment of rosette leaves of transgenic plants shown in *A*, arranged left to right from first to last leaves to emerge. (*C*) Distribution of rosette size in the T1 generation of transgenic plants. The number of plants observed is 71 (AC), 64 (AS), 48 (AS35), 35 (C), and 51 (S). The maximum rosette size was measured at 50–60 days after sowing. (*D*) Growth kinetics of T2 plants. Each curve represents an independent transgenic line, and each data point is the average of measurements from 7 to 10 plants. The maximum rosette sizes of the T1 lines selected for this T2 analysis (also for Table 1) were 4–6 cm for AS lines, 3–6 cm for AC lines, 2–5 cm for AS35 lines, 9–11 cm for S lines, and 8–9 cm for the C line. Col, Columbia wild type.

Table 1. Leaf dimension of transgenic plants

Constructs*	n	Blade length, mm	Blade width, mm	Petiole length, mm
AS	24	18.5 ± 3.4 (77)	14.8 ± 2.5[†] (95)	5.7 ± 1.7 (59)
AC	29	18.8 ± 3.9 (78)	13.3 ± 2.7 (85)	6.2 ± 1.9 (64)
AS35	27	13.6 ± 3.9 (56)	10.9 ± 3.0 (70)	5.1 ± 1.8 (53)
C	17	24.1 ± 1.6 (100)	15.6 ± 1.8 (100)	9.7 ± 1.5 (100)
S	27	27.8 ± 2.7 (115)	17.2 ± 1.8 (110)	12.3 ± 1.5 (127)

The eighth leaf from 32-day-old plants was used. Values are averages ± SD. Percentages indicated in parentheses after each value are relative to control values. Averages are significantly different from control at $P < 0.05$, except for †, where $P = 0.078$. n, sample number.
*For each construct, two to three independent T2 lines (7–10 plants for each line) were observed.

for most of the differences in petiole length. The physical basis for these growth changes was further explored in extensometer assays, which revealed a marked reduction in the extensibility of petiole cell walls from antisense plants (Fig. 6). This result is consistent with reduced expansin activity in the antisense plants. Cell walls from the sense plants showed slightly faster extension in the first 30 min of the assay, but this was not statistically significant, probably because of the smaller growth effect seen in sense plants. These data on cell size and wall extension are consistent with the hypothesis that AtEXP10 influences leaf growth through its effects on cell-wall rheology.

In addition to smaller leaves, the majority of antisense plants showed variable degrees of leaf twisting and bending along the midrib and edges (Fig. 5 A and B). The aberrant morphology generally appeared after the fifth or sixth leaf (Fig. 5B) and later-stage leaves showed more severe phenotype. The AC construct resulted in the highest proportion (90%) of the plants with twisted leaves, but the most severe phenotype was more abundant in the AS population. The slightly different morphology of AC plants as compared with AS plants may have resulted from antisense effects on other expansin genes by the AC construct, which contains the conserved coding region for expansin. In the AS35 population, 50% had normal flat leaves, albeit smaller than wild type. Sense, control, or wild-type plants rarely had twisted leaves.

AtEXP10 Affects Pedicel Abscission.

Because *AtEXP10* is expressed at the base of the pedicel, which resembles a vestigial abscission zone (Fig. 2D), we investigated the impact of *AtEXP10* overexpression and suppression on pedicel abscission. Because this anatomical region is not a physiologically genuine abscission zone in *Arabidopsis* (it does not spontaneously abscise), we used force to identify the weak point of the pedicel by the location of pedicel breakage. In control plants, the older pedicels mostly broke in the middle of the pedicel ("incomplete abscission"; Fig. 7), whereas the young pedicels showed a clean, or "complete," breakage at the base. The breakage at the base of the pedicel correlates with the endogenous expression of *AtEXP10*, which decreases as the siliques mature (Fig. 3A). In *AtEXP10* antisense plants, the young pedicels had a lower incidence of complete (clean) breakage than did controls, whereas in sense plants the older pedicels had a higher incidence of complete

breakage than did controls (Fig. 7). These results show that the pattern of pedicel breakage can be altered by manipulation of *AtEXP10* expression.

Discussion

Expansins and Growth. Expansins are thought to function in the control of plant cell growth on the basis of three lines of evidence: (*i*) they loosen cell walls *in vitro* (8); (*ii*) they stimulate cell enlargement when applied exogenously (9, 10); and (*iii*) they are expressed in a pattern that is consistent with their involvement in growth (11–13, 16). In this study, we carried out a transgenic test for the endogenous function of a specific expansin gene (*AtEXP10*) in transgenic Arabidopsis plants by manipulating its expression with tissue-specific and gene-specific constructs.

Leaf size was substantially reduced in antisense lines with suppressed *AtEXP10* expression, whereas overexpression of *AtEXP10* resulted in plants with somewhat larger leaves. These changes in petiole length were correlated with changes in cell size. Furthermore, a marked reduction in acid-induced cell-wall extension (creep) *in vitro* was observed in walls from the petioles of antisense plants. These results indicate that *AtEXP10* specifically functions in the control of leaf size in *Arabidopsis* through its action on cell-wall rheology and, more generally, support the hypothesis that the wall-loosening activity of expansin is an important control point for the regulation of plant cell growth.

Because *AtEXP10* is preferentially expressed in the petiole and the midrib, it is perhaps surprising that growth of the leaf blade was altered to nearly the same extent as that of the petiole and midrib. One possible explanation is that growth of the blade is coordinated with midrib growth, either through direct mechanical effects mediated by adhesion between cells or through more indirect mechanisms coordinating midrib elongation with blade growth (25). Leaf twisting along the midrib in the *AtEXP10* antisense lines may result from imperfect coordination between midrib and blade growth. In the tobacco *lam-1* mutant, which is defective in blade growth because of the lack of blade meristematic activity (26), the mutant leaves are rod-shaped but of normal length. The midrib thus seems to be a determining structure in leaf ontogeny, and its growth may be decisive for leaf length. Additionally, low-level expression of the *AtEXP10* pro-

Table 2. Petiole length, number of cells per cell file, and cell length in transgenic plants

Construct*	n	Petiole length, mm	Cell number	Cell length, μm
Control	10	8.6 ± 1.6 (100.0)	31.3 ± 4.3 (100.0)	271 ± 33 (100.0)
Sense	9	9.4 ± 1.5 (109.3)[†]	31.4 ± 3.9 (100.3)[†]	298 ± 41 (110.0)[‡]
Antisense	10	7.0 ± 1.4 (81.4)[‡]	33.5 ± 5.2 (107.0)[†]	207 ± 27 (76.4)[‡]

Petioles were from 27-day-old fifth leaves of T3 plants. Cells were counted in subepidermal cell files on the abaxial surface of the petiole. Values are averages ± SD. Percentages indicated in parentheses after each value are relative to control values. n, sample number.
*Transgenic lines were C12-5 (control), S9-1 (sense), and AS13-1 (antisense).
†Not significantly different from control.
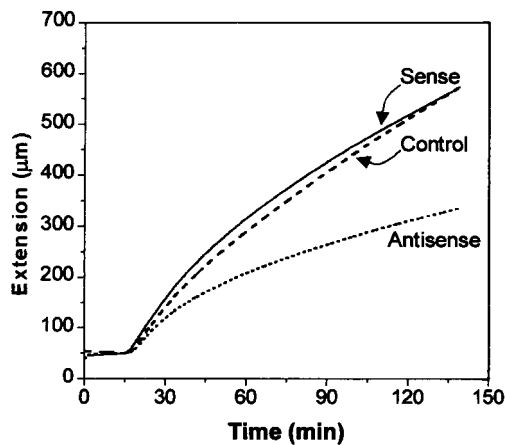‡Significantly different from control at $P < 0.05$.

Fig. 6. Extension of cell walls from growing petioles of transgenic plants. Native wall specimens from the seventh leaf of 29-day-old T3 plants were clamped at constant load, initially in 50 mM Hepes buffer, pH 6.8, and at 15 min the buffer was exchanged for 50 mM sodium acetate, pH 4.5, to activate expansin-induced extension. These curves are the averages of four, eight, or nine samples for control (C12–5 line), antisense (AS13–1), and sense (S9–1) plants. The antisense curve was significantly different from the control and sense curves (Student's *t* test, $P < 0.05$).

Fig. 7. Pattern of pedicel abscission in transgenic plants. Abscission was evaluated as percentage of incomplete abscission where breakage occurs in the middle of pedicel instead of at the exact abscission region. Data are from 21 plants (from four independent lines) for AC, 9 plants (from one line) for C, and 23 plants (from four independent lines) for S. (*Inset*) Depiction of the breakage pattern seen with incomplete or complete abscission.

moter in the shoot apical meristem and in the leaf blade may have influenced blade growth.

Expansin and Pedicel Abscission. Shedding of plant organs is normally achieved by differentiation of an abscission zone, where localized cell expansion, wall breakdown, and cell separation occur (27). Although *Arabidopsis* lacks a morphologically distinct abscission zone at the base of the pedicel, this may be a recently derived condition, because in many plants the base of the pedicel contains a functional abscission zone (27). The expression of *AtEXP10* in the pedicel base may be a vestige of an evolutionarily lost abscission zone in this area. Expansins may contribute to abscission by modifying cell walls to enhance cell separation, as well as by inducing expansion of cells on the proximal face of the abscission zone, giving rise to a mechanical force to push away the shedding organ (27). The abscission results with *AtEXP10* antisense plants are similar to those reported for antisense suppression of endo-1,4-β-glucanase in tomato fruit abscission zones (5). Although *AtEXP10* is not expressed in true abscission zones of *Arabidopsis* (e.g., at the bases of flower petals and mature siliques), expression
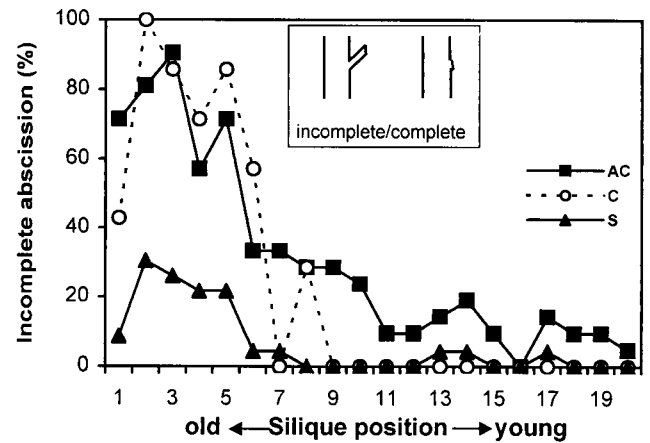
of other expansin genes is specifically increased in these regions just before abscission (D. M. Durachko and D.J.C., unpublished results). Our results imply a cell-separation function for these expansin genes.

In summary, genetic manipulation of *AtEXP10* expression indicates that a major biological role of this expansin is in control of leaf growth. Our results are consistent with results from transgenic rice plants, where modification of expansin expression affects plant stature and leaf initiation (H. Kende, personal communication). In addition to a role in leaf growth, *AtEXP10* also influences the mechanical breakage behavior of the pedicel, perhaps as a vestige of a now-lost abscission zone at the base of the pedicel. If this phenomenon is common to abscission and dehiscence zones in other species, genetic manipulation of expansin gene expression may find new applications in controlling fruit drop, seed pod shatter, and flower petal abscission.

1. Cosgrove, D. J. (1999) *Annu. Rev. Plant Physiol. Plant Mol. Biol.* **50,** 391–417.
2. Carpita, N. C. & Gibeaut, D. M. (1993) *Plant J.* **3,** 1–30.
3. Gonzalez-Carranza, Z. H., Roberts, J. A. & Lozoya-Gloria, E. (1998) *Trends Plant Sci.* **3,** 10–14.
4. Rose, J. K. C. & Bennett, A. B. (1999) *Trends Plant Sci.* **4,** 176–183.
5. Brummell, D. A., Hall, B. D. & Bennett, A. B. (1999) *Plant Mol. Biol.* **40,** 615–622.
6. McQueen-Mason, S. & Cosgrove, D. J. (1995) *Plant Physiol.* **107,** 87–100.
7. Li, Z.-C., Durachko, D. M. & Cosgrove, D. J. (1993) *Planta* **191,** 349–356.
8. McQueen-Mason, S., Durachko, D. M. & Cosgrove, D. J. (1992) *Plant Cell* **4,** 1425–1433.
9. Link, B. M. & Cosgrove, D. J. (1998) *Plant Physiol.* **118,** 907–916.
10. Fleming, A. J., McQueen-Mason, S., Mandel, T. & Kuhlemeier, C. (1997) *Science* **276,** 1415–1418.
11. Shcherban, T. Y., Shi, J., Durachko, D. M., Guiltinan, M. J., McQueen-Mason, S., Shieh, M. & Cosgrove, D. J. (1995) *Proc. Natl. Acad. Sci. USA* **92,** 9245–9249.
12. Cho, H.-T. & Kende, H. (1997) *Plant Cell* **9,** 1661–1671.
13. Cho, H.-T. & Kende, H. (1998) *Plant J.* **15,** 805–812.
14. Fleming, A. J., Caderas, D., Wehrli, E., McQueen-Mason, S. & Kuhlemeier, C. (1999) *Planta* **208,** 166–174.
15. Rose, J. K. C., Lee, H. H. & Bennett, A. B. (1997) *Proc. Natl. Acad. Sci. USA* **94,** 5955–5960.
16. Hutchison, K. W., Singer, P. B., Diaz-Sala, C. & Greenwood, M. S. (1999) *Plant Physiol.* **120,** 827–832.
17. Cosgrove, D. J. (2000) *Curr. Opin. Plant Biol.* **3,** 73–78.
18. Krysan, P. J., Young, J. C. & Sussman, M. R. (1999) *Plant Cell* **11,** 2283–2290.
19. Becker, D., Temper, E., Schell, J. & Masterson, R. (1992) *Plant Mol. Biol.* **20,** 1195–1197.
20. Bechtold, N. & Pelletier, G. (1998) in *Arabidopsis Protocols*, eds. Martinez-Zapater, J. M. & Salinas, J. (Humana, Totowa, NJ), pp. 259–266.
21. Cosgrove, D. J. (1989) *Planta* **177,** 121–130.
22. Behringer, F. J., Cosgrove, D. J., Reid, J. B. & Davies, P. J. (1990) *Plant Physiol.* **94,** 166–173.
23. Freeman, W. M., Walker, S. J. & Vrana, K. E. (1999) *BioTechniques* **26,** 112–115.
24. Nellen, W. & Lichtenstein, C. (1997) in *Antisense Technology*, eds. Lichtenstein, C. & Nellen, W. (Oxford Univ. Press, New York), pp. 25–38.
25. Scanlon, M. J. (2000) *Curr. Opin. Plant Biol.* **3,** 31–36.
26. McHale, N. A. & Marcotriagno, M. (1998) *Development (Cambridge, U.K.)* **125,** 4235–4243.
27. Addicott, F. T. (1982) *Abscission* (Univ. of California Press, Berkeley).